RESEARCH ARTICLE | AUGUST 08 2014

Hydrogen migration in formation of NH($A\,^3\Pi$) radicals via superexcited states in photodissociation of isoxazole molecules

Mariusz Zubek; Tomasz J. Wasowicz; Iwona Dąbkowska; Antti Kivimäki; Marcello Coreno

J. Chem. Phys. 141, 064301 (2014)
https://doi.org/10.1063/1.4891808

Hydrogen migration in formation of NH($A^3\Pi$) radicals via superexcited states in photodissociation of isoxazole molecules

Mariusz Zubek,[1,a)] Tomasz J. Wasowicz,[1] Iwona Dąbkowska,[2] Antti Kivimäki,[3,4] and Marcello Coreno[4,5]
[1]*Department of Physics of Electronic Phenomena, Gdańsk University of Technology, 80-233 Gdańsk, Poland*
[2]*Department of Chemistry, University of Gdańsk, 80-952 Gdańsk, Poland*
[3]*CNR-IOM, Laboratorio TASC, 34149 Trieste, Italy*
[4]*Gas Phase beamline@Elettra, Basovizza Area Science Park, 34149 Trieste, Italy*
[5]*CNR-IMIP, Monterotondo, 00016 Roma, Italy*

(Received 26 May 2014; accepted 20 July 2014; published online 8 August 2014)

Formation of the excited NH($A^3\Pi$) free radicals in the photodissociation of isoxazole (C_3H_3NO) molecules has been studied over the 14-22 eV energy range using photon-induced fluorescence spectroscopy. The NH($A^3\Pi$) is produced through excitation of the isoxazole molecules into higher-lying superexcited states. Observation of the NH radical, which is not a structural unit of the isoxazole molecule, corroborates the hydrogen atom (or proton) migration within the molecule prior to dissociation. The vertical excitation energies of the superexcited states were determined and the dissociation mechanisms of isoxazole are discussed. The density functional and *ab initio* quantum chemical calculations have been performed to study the mechanism of the NH formation. © *2014 AIP Publishing LLC*. [http://dx.doi.org/10.1063/1.4891808]

I. INTRODUCTION

Electronic excitation of hydrocarbon molecules can initiate their isomerization, which is a process leading to substantial rearrangement deformation of the molecular bond structure. Subsequently, isomerization may lead to opening of new reaction channels, which frequently include dissociation. In cyclic hydrocarbons, absorption of radiation can trigger opening of the ring molecular structure, which will be followed by fragmentation of its open chain isomer. In this rearrangement, the ultrafast intramolecular migration of hydrogen atoms (protons) from one site of the molecule to another plays an important role.[1–3] It occurs on a femtosecond time scale in the ground and excited states and is faster than the molecular bond breaking in dissociation. The characteristics of the hydrogen migration have been revealed in the studies of acetylene, a simple hydrocarbon molecule, which serves as a model for 1,2 hydrogen migration from one carbon atom to the other. This isomerization transition between the linear acetylene (HCCH) and planar vinylidene (H_2CC) structures has been studied experimentally and theoretically in neutral acetylene,[4–7] its cations,[8–10] and dications.[11–14] While the studies of a neutral acetylene most commonly focused on the energy states of the isomerizing species and energetics of the reaction (transition states, barriers),[5,7] the studies of cations and dications allowed to investigate the hydrogen migration dynamics. Observation of the two-body Coulomb explosion in the intense laser fields (10^{13}–10^{15} W/cm^2) by applying the coincidence momentum imaging method[15] delivered information on the molecular structure of the dications just before the Coulomb explosion.[13,14] The hydrogen migration (isomerization) time in mono- and dications of acetylene was found at 50–60 fs[9,11] and migration appeared as a recurrent process of oscillations between the acetylene and vinylidene structures.[10,13] The hydrogen migration has also been investigated in more complex hydrocarbon molecules.[3,16–23] In the open chain hydrocarbons, studied most often in intense laser fields, mechanism and the time scale of the 1,2 hydrogen migration processes between two adjacent carbon atoms[3,16–20] is, in general, similar to that of acetylene. However, the range of migration may extend beyond the two adjacent carbon atoms as, for example, in allene CH_2=C=CH_2, where the hydrogen transfer covers the entire length of the molecule (1,3 hydrogen migration).[18] In the cyclic hydrocarbons, the hydrogen migration has been observed in the closed ring structures within pericyclic reactions in the neutral molecules excited to lower-lying states.[21–23] However, the ring opening mechanism and the following hydrogen migration in the open chain parent hydrocarbon molecule may also occur as it was assumed, for example, in cyclohexane cations.[3]

In the present work, we have investigated photodissociation of the isoxazole (C_3H_3NO) molecules, which results in formation of the excited NH($A^3\Pi$) molecular fragments. Isoxazole is a five-membered planar heterocyclic compound incorporating adjacent to each other one nitrogen and one oxygen heteroatom (Fig. 1). The outermost occupied molecular orbitals of the X^1A' ground state of isoxazole are $(11a')^2(1a'')^2(12a')^2(13a')^2(14a')^2(15a')^2(2a'')^2(3a'')^2$. The 15a′ orbital is the σ nitrogen lone pair (LP_N) and the 1a″, 2a″, and 3a″ orbitals are labeled π_1, π_2, and π_3, respectively. Isoxazole has found various pharmacological (antibacterial, antiallergic) and agrochemical (herbicidal, insecticidal) applications.[24] In recent years isoxazole molecule has become a subject of an increased laboratory research, because it may serve as a simple analogue of the components of the

a)Electronic mail: mazub@mif.pg.gda.pl

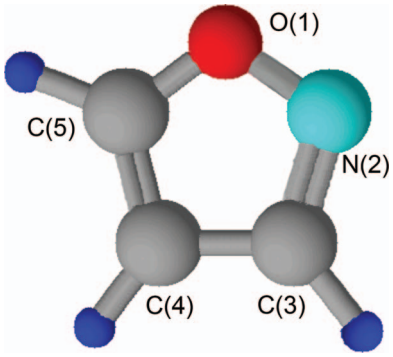

FIG. 1. Schematic diagram of the isoxazole molecule, C_3H_3NO, showing labelling of the atoms. Color code: the carbon atom is grey, oxygen atom is red, nitrogen atom is blue, hydrogen atom is dark blue.

nucleic acids bases in DNA in the investigations of interaction of the ionizing radiation on the biological tissue. For example, adenine and guanine, in their five-membered molecular subrings contain nitrogen atoms. The impact of the energetic primary radiation and the secondary species, chemically active cations, free radicals, and ballistic secondary electrons induces structural alterations in the molecular units of the DNA helix by bond cleavages.[25,26] These alterations promote mutagenic and carcinogenic ramifications, which ultimately may lead to cellular death. Studies of the fragmentation processes in the prototypes of the DNA units induced by photon and charge particle impact provide insight on the molecular level into the bond cleavage mechanisms. These studies have also more general purpose of research of the dissociation reactions, for example, in the molecules adsorbed on the surface in the focused electron beam induced deposition technique.

Previously, fragmentation of isoxazole molecules was explored predominantly by pyrolysis techniques. In these studies, a single-pulse shock tube reactor over the 850–1100 K temperature range[27] and flash vacuum pyrolysis (620–1170 K)[28] were used. Very recently, a high-pressure pulsed pyrolysis was applied, where the fragmentation products were isolated in the argon matrix at 10–20 K and analyzed by IR vibrational spectroscopy.[29] It was found that the major products of the thermal decomposition were acetonitrile $CH_3C{\equiv}N$ and carbon monoxide CO accompanied by several minor products, which included hydrogen cyanide HCN, ketene CH_2CO, and acetylene C_2H_2 molecules.[27] The high-pressure pulse pyrolysis[29] produced ketenimine $H_2C{=}C{=}NH$ and CO. These experimental studies were followed by quantum chemical calculations of the fragmentation processes.[29–31] The density functional calculations[31] indicated that before decomposition the isoxazole molecule may be a subject of intense isomerization processes involving ring opening and hydrogen migrations. It was further supported by calculations in Refs. 29 and 32 that the nitrile isomer $N{\equiv}CCH_2CHO$ formed by cleavage of the weak N–O bond and 1,2 hydrogen migration from C(3) to C(4) is a stable intermediate undergoing further rearrangement in decomposition into acetonitrile $CH_3C{\equiv}N + CO$ or ketenimine $H_2C{=}C{=}NH + CO$. This intermediate state is separated from the initial ring conformation and the final decomposition products by potential energy barrier of about 3.5 and 3.1 eV, respectively.[29,31,32] Recently, the photo[33] and electron impact[34] fragmentation of isoxazole molecules producing excited atomic and diatomic fragments was investigated using the fluorescence spectroscopy in the 16–50 eV and 10–90 eV energy range, respectively. The following species were detected, H(n), n = 3–7, CH($A^2\Delta$, $B^2\Sigma^-$), CN($B^2\Sigma^+$), and $C_2(d^3\Pi_g)$, which occur following excitation of the isoxazole molecules into the superexcited states.

In this study, we report results on photodissociation of the isoxazole molecules into the excited NH($A^3\Pi$) radicals in the 14–22 eV photon energy range. The NH radicals were observed by detecting emission of the $A^3\Pi \rightarrow X^3\Sigma^-$ system, applying photon-induced fluorescence spectroscopy (PIFS). It is found, as observed in our work earlier,[33] that the isoxazole molecules are excited into the higher-lying superexcited states, which are subject to internal rearrangement prior to dissociation. The NH radical is not a structural unit of the isoxazole molecule and its identification within the dissociation products gives an evidence of the hydrogen migration during rearrangement reaction. To further study the mechanism of the NH formation we have performed the density functional and *ab initio* quantum chemical calculations, which demonstrated that the hydrogen migration mechanism may be determined by the ion core binding the excited Rydberg electron in the superexcited state of the molecule.

II. EXPERIMENTAL

The experiment was carried out at the Gas-Phase Photoemission beamline of the Elettra synchrotron radiation facility at Trieste. Radiation delivered by a 36-period undulator was dispersed by a spherical grating monochromator. The grating G6 covering the energy range 14–28 eV was used in the experiment. The photon energy scale was calibrated against the selected valence excitation lines in noble gases and nitrogen to better than ±20 meV. The contribution of the second order light in the 14–22 eV energy range is considered to be ≤5%.

The PIFS setup that was used in the present studies is shown schematically in Fig. 2. The effusive beam of the isoxazole vapour from a hypodermic needle intersected the monoenergetic photon beam delivered by the beamline. Fluorescence emitted by the dissociation fragments from the interaction region was reflected and collimated by a spherical mirror in the direction parallel to polarization vector of the synchrotron radiation. The position of the mirror was carefully adjusted to maximize the detected fluorescence intensity. The interaction region had an estimated cylindrical shape of 0.4 mm diameter and 1–2 mm length, depending on the width of the entrance slit of the optical spectrograph used in the detection channel. From the size of the spherical mirror, it is evaluated that about 10% of the total fluorescence from the interaction region emitted in a narrower viewcone is projected onto the entrance slit of the spectrograph. This collection geometry would not introduce any angular emission effects, as the fluorescence from the dissociated NH($A^3\Pi$) fragments is expected to have isotropic angular distribution due to rotational motion of the fragments. The collimated fluorescence beam was focused on the entrance slit of the 0.5 m Minuteman 305 MV spectrograph equipped with a 1200 lines/mm grating blazed at 500 nm. The dispersed fluorescence

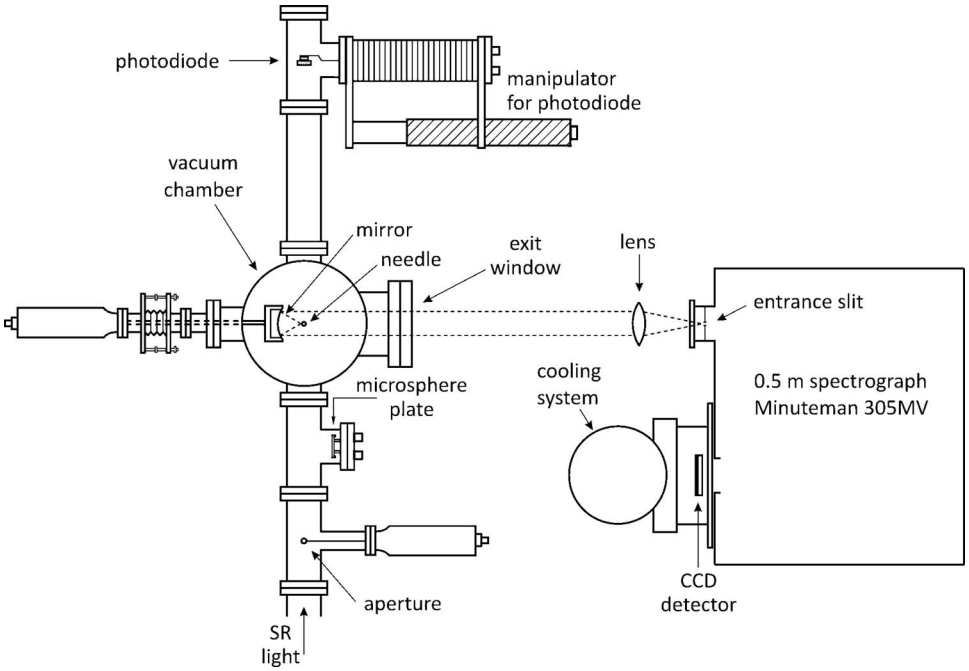

FIG. 2. Schematic view of the experimental arrangement.

spectra were recorded in a wavelength window of 40 nm by a CCD detector (Princeton 10:100B) cooled by liquid-nitrogen to about −170 K. These spectra were corrected for the wavelength variation of sensitivity of the detection channel applying sensitivity curve determined previously.[35] The incident photon flux, estimated at $\sim 10^{13}$ photons/s, was monitored during acquisition of the spectra by a calibrated photodiode, mounted on a manipulator at the end of the vacuum chamber. The photodiode current was utilized for normalization of the spectra to constant photon flux. The experimental system was also equipped with a microsphere plate, in order to additionally record cationic current from ionization of the target molecules. The pressure in the target molecular beam is estimated to be ∼30 times higher than that in the vacuum vessel, which was 7×10^{-4} mbar. The linear dependence between detected signal and the isoxazole vapour pressure was maintained throughout the measurements.

The fluorescence spectra of the NH $A^3\Pi \rightarrow X^3\Sigma^-$ system were recorded in the 325–346 nm window in the 14–22 eV photon energy range with a 0.25 eV step. The spectra were calibrated against the position of the H_γ Balmer line at 434.0 nm to within ±0.1 nm. The background level in the spectra was verified by cutting off the incident photon beam and was subtracted from the recorded spectra. More details on the present experimental procedure may be found in Ref. 35 and on PIFS method to investigate the superexcited states in Ref. 36.

The liquid isoxazole sample was purchased from Sigma-Aldrich Chemie with a declared purity of 99%. It was purified in a sample container by applying freezing-pumping-thawing cycles to remove any contaminating gases. The isoxazole vapour was introduced into the hypodermic needle through a stainless steel gas inlet system. The vapour pressure of isoxazole at room temperature is high enough and the studies were carried out without heating the sample.

III. THEORETICAL METHODS

To provide more insight into the energy barriers for opening of the isoxazole ring and, in particular, into migration of hydrogen (proton) the density functional and *ab initio* quantum chemical calculations have been carried out for both, the neutral molecule and the lowest energy cation $(3a'')^{-1}$ A″ of isoxazole. The initial structures of the cationic and neutral tautomers of isoxazole were calculated with the B3LYP/6-311++G(d,p) method.[37,38] Then the geometries were re-optimized at the level of the second-order Møllet-Plesset perturbation theory (MP2)[39] with the same basis set. No geometry constrains were imposed at this stage of the calculations and the analysis of the harmonic vibrational frequencies confirmed their geometrical stability. The calculated neutral geometry equilibrium bond length and angles are in very good agreements with previous computations[40] and the vibrational frequencies, when scaled down using scaling factor of 0.95 are in agreement with the experimental and theoretical data.[41] In order to provide a more complete description of the target molecule, the ionization potentials were computed for the neutral ring geometry using the outer-valence Green's functions propagator (OVGF).[42] The obtained ionization potentials for orbitals of interest, 3a″ (9.962 eV), 13a′ (14.562 eV), and 12a′ (15.679 eV) are in excellent agreement with the measured values.[43,44]

Investigations of the hydrogen migration have been carried out by a number of optimization calculations performed for the $(3a'')^{-1}$ A″ cationic structures, where the selected N–O distances were frozen, while the other coordinates were unconstrained. These geometries of isoxazole with increasing N–O distances served as a model of ring opening mechanism to investigate the dynamics of hydrogen migration. As a starting point, the fully optimized cationic ring structure, with the equilibrium N–O bond length of 1.4965 Å was used.

All these calculations were done at the MP2/6-311++G(d,p) level of theory. They were complemented by determination of the transition state (TS) in two approaches: (1) using the guessed geometry of a TS, (2) direct optimization to a maximum on the potential energy surface by Berny's algorithm,[45] and by implementing "Synchronous Transit-Guided Quasi-Newton" method.[46] Both methodologies led to the same structure of the TS, which was further confirmed by analysis of the vibrational frequencies.

The dissociation energy for the C≡N bond cleavage in the open ring isoxazole molecule was calculated on electronic energy scale, as a difference between the energy of the open-ring neutral tautomer and the sum of energies of isolated molecular fragments (OCHCHC and NH), both fully optimized into their triplet configurations.

All computations were performed using the GAUSSIAN G03 package.[47]

IV. RESULTS AND DISCUSSION

The emission spectrum of the NH $A^3\Pi \rightarrow X^3\Sigma^-$ system measured in the 325–346 nm range, at the photon energy of 17.5 eV, with a resolution of the optical spectrograph $\Delta\lambda$ of 0.5 nm (FWHM) is shown in Fig. 3. The lines of the P, Q, R rotational branches of the detected (0,0) and (1,1) vibrational bands, observed in Ref. 48, are also indicated. The Q branches in the (0,0) and (1,1) bands give intensity maxima at 336.2 and 337.4 nm, respectively, while the other branches appear as wings below and above the maxima. The intensity ratio of the (1,1) to (0,0) band, determined from fitting the measured spectrum, is 0.67. The best fit (not shown in Fig. 3) was obtained for the temperature of 8000 K of the Boltzmann distribution assumed for the rotational level population. Moreover, it was found that the intensity ratio and the rotational temperature stayed unchanged in the studied 14–22 eV photon energy range. The clear observation of the NH fragment demonstrates the hydrogen (proton) atom migration within the isoxazole molecule prior to dissociation.

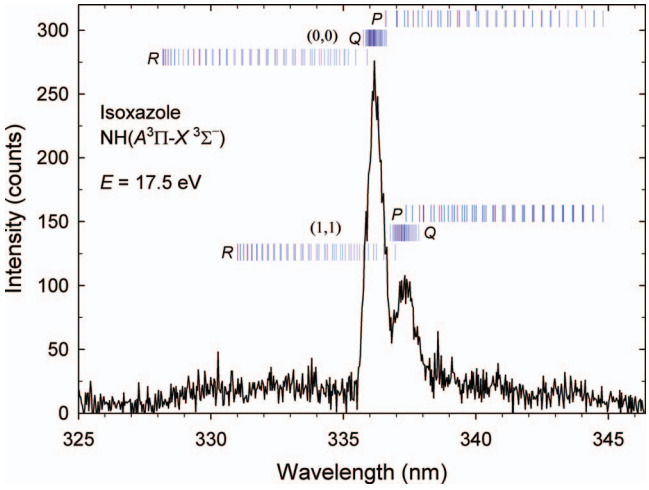

FIG. 3. Fluorescence spectrum of the isoxazole molecules measured in the wavelength range 325–346 nm, at a photon energy of 17.5 eV. Positions of the rotational lines of the Q, P, R branches of the (0,0) and (1,1) bands of the NH $A^3\Pi \rightarrow X^3\Sigma^-$ system are indicated by vertical bars.

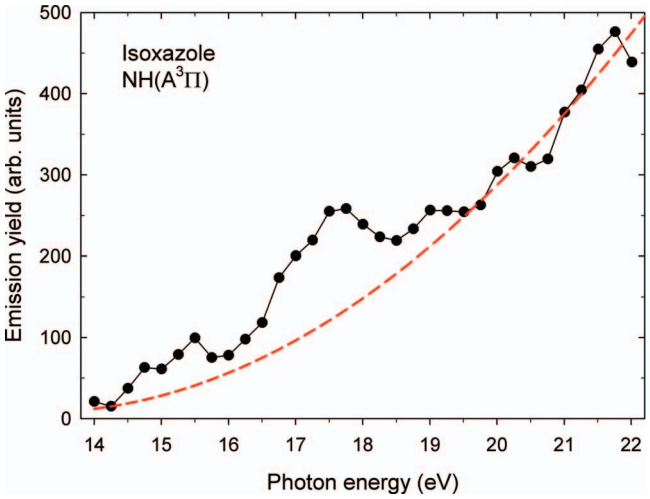

FIG. 4. The NH ($A^3\Pi$) photodissociation yield obtained in isoxazole in the 14–22 eV photon energy range. The dashed line shows the fitted (19.5–22 eV) and extrapolated (14–19.5 eV) parts of the curve corresponding to the overlapping unresolved features in the dissociation yield.

The photodissociation yield curve for formation of the NH($A^3\Pi$) radicals in the 14–22 eV range is shown in Fig. 4. The curve was obtained by integrating the $A^3\Pi \rightarrow X^3\Sigma^-$ spectra in the 328–346 nm wavelength range at each photon energy. The statistical uncertainty in the emission yield in Fig. 4 is not larger than ±5%. The yield curve increases from a threshold at about 14 eV and in the energy range up to about 19.5 eV displays maxima superimposed on a steady rising background. Above 19.5 eV it continues to rise showing weaker structures on the background. The maxima have the form of the overlapping bands corresponding to excitation of the higher-lying states of isoxazole, the superexcited states, which dissociate producing the excited NH($A^3\Pi$) radicals. The rising background is ascribed to overlapping features not discerned in the emission yield. The superexcited states are inner-valence Rydberg or multiply excited electronic states, whose energies considerably exceed the first ionization potentials.[49,50] They decay preferentially through nonradiative routes: dissociation or, competing with it, autoionization.[51] To determine the contribution of the superexcited states, the yield curve was fitted with a function of quadratic energy dependence in the 19.5–22 eV range and extrapolated down to lower energies. The quadratic energy dependence obtained in the 19.5–22 eV when extrapolated down to lower energies converge on the threshold at about 14 eV. Next, the extrapolated function was subtracted from the dissociation yield curve to obtain intensity due to excitation of the superexcited states, which is shown in Fig. 5.

The vertical excitation energies of the observed superexcited states were attained by deconvoluting the yield curve of Fig. 5 into the individual excitation bands. Here, a least-squares fitting procedure was applied, where the shapes of the excitation bands were described by the Gaussian profiles. The fitting procedure allowed the energies and widths of the bands to be optimized simultaneously. The Lorentzian profiles, when used in the fitting, did not give the same exact reproduction of the measured dissociation yield curve. The

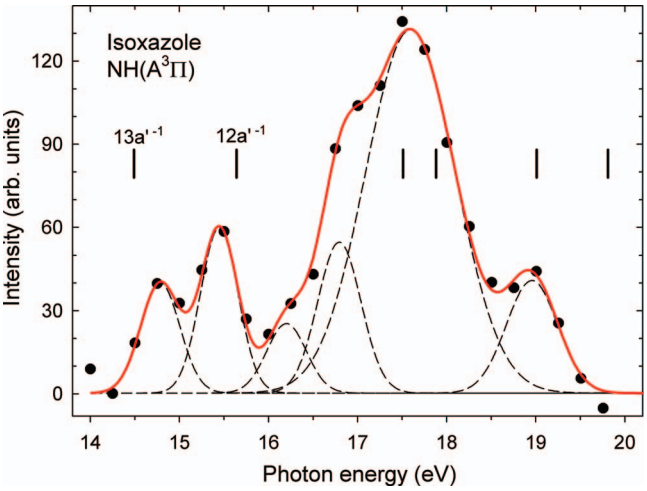

FIG. 5. The NH ($A^3\Pi$) photodissociation yield corresponding to the overlapping bands of the superexcited states. The bands fitted to the experimental curve are shown by the dashed lines and the final fit is shown by the solid line. The ionization vertical energies of the ion core molecular orbitals are indicated by vertical bars.

excitation bands are shown by the dashed lines in Fig. 5 together with the final fit to the yield curve. The vertical excitation energies (centers of the bands) and widths of the bands are listed in Table I. The present energies are compared in Table I with those found in a previous study[33] from our group of photodissociation of isoxazole into the CH($A^2\Delta$) fragments. In Fig. 5 and Table I, the ionization energies from the respective ion core molecular orbitals and widths of the measured photoelectron bands[43,44] are also included to correlate tentatively the superexcited states with their likely ionic cores.[52] For example, the superexcited states at 14.8 and 15.45 eV are placed below the $(12a')^{-1}$ ion core energy (15.64 eV). Furthermore, the widths of the bands of these superexcited states coincide with that of the $(12a')^{-1}$ photoelectron band. Therefore, the two superexcited states may be considered as the Rydberg states built on the $(12a')^{-1}$ ion core, with binding energies of 0.8 and 0.2 eV, respectively. In a similar way, the 16.2 and 16.8 eV states may be attributed to the $11a'^{-1}$ (leading open shell orbital) ionic core (17.88 eV) with slightly higher binding energies of 1.7 and 1.1 eV, respectively.

TABLE I. The vertical excitation energies of the superexcited states of the isoxazole molecules, widths of the excitation bands, ionization energies of the indicated ion core molecular orbitals, and widths of the measured photoelectron bands.

Superexcited state			Photoelectron band		
Energy (eV)[a]	Width (eV)[a]	Energy (eV)[b]	Energy (eV)	Width (eV)	Ion core[c]
			19.81[d]	1.3[d]	
19.0 ± 0.1	0.7	19.2 ± 0.4	19.01[d]	0.6[d]	
		18.4 ± 0.5			
			17.88[d]	0.5[d]	$(11a'^{-1})$[e]
17.6 ± 0.1	1.2	17.6 ± 0.3			
			17.51[d]	1.5[d]	$(1a''^{-1})$[e]
16.80 ± 0.15	0.6	16.8 ± 0.5			
16.2 ± 0.3	0.5				
			15.64[f]	0.6[f]	$12a'^{-1}$
15.45 ± 0.05	0.5				
14.8 ± 0.1	0.5				
			14.49[d]	0.75[d]	$13a'^{-1}$

[a]Present.
[b]Reference 33.
[c]Reference 52.
[d]Reference 44.
[e]Leading open shell orbital from Ref. 52.
[f]Reference 43.

The observed superexcited states are the door-states in dissociation of the isoxazole molecules into NH($A^3\Pi$). The cyclic structure of isoxazole implies a fragmentation reaction, which proceeds through ring opening by cleavage of the weak N–O bond. This is an accepted initial step for isoxazole dissociation.[29] The nonadiabatic photoinduced ring opening in the lowest excited singlet states was predicted in furan, which is isoelectronic to isoxazole, in *ab initio* quantum dynamical calculations and expected to be of relevance in other five-membered heterocycle molecules.[53] This will be followed by hydrogen migration from C(3) to N(2) in isoxazole that builds the NH diatomic fragment as terminating the molecular open chain (Fig. 6). Finally, the excited NH fragment detaches from the chain by scission of the C≡N bond. Alternatively, the superexcited states may undergo transition on the femtosecond time scale through internal conversion to lower lying states.[54] Those lower lying states, again of Rydberg character, will dissociate yielding the NH fragments. Because the Rydberg electrons are weakly bound and have larger orbital radius, the rearrangement and dissociation dynamics will be mainly governed by that of the ionic cores of the superexcited states.

The initial state in the photoabsorption process is the neutral state of isoxazole molecule, while the superexcited state is the Rydberg state with the $(3a'')^{-1}$ ion core. The analyses of the fully optimized geometries of the neutral and cationic states show that removal of the 3a″ electron significantly increases the N–O distance (from 1.394 to 1.496 Å) and C(4)-C(5) distance (from 1.366 to 1.442 Å) while decreasing the C(5)–O(1) bond length (from 1.356 to 1.282 Å) and N(2)-C(3) (from 1.330 to 1.282 Å). These changes can be explained by rendering the molecular orbitals. The 3a″ orbital charge distribution localizes mainly on the C(4)-C(5) bond and N atom. Studies of the hydrogen migration have been performed for the $(3a'')^{-1}$ A″ cationic structures, where the selected N–O distances were frozen, while the other coordinates were unconstrained. The schematic geometries and the energies of the planar cationic structures obtained in the calculations, related to that of the closed ring of isoxazole cation (absolute electronic energy of −244.9670514 hartree),

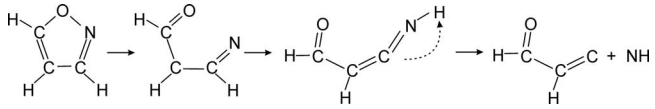

FIG. 6. Schematic view of the dynamics of isoxazole molecules dissociation drawn using ChemSketch program.

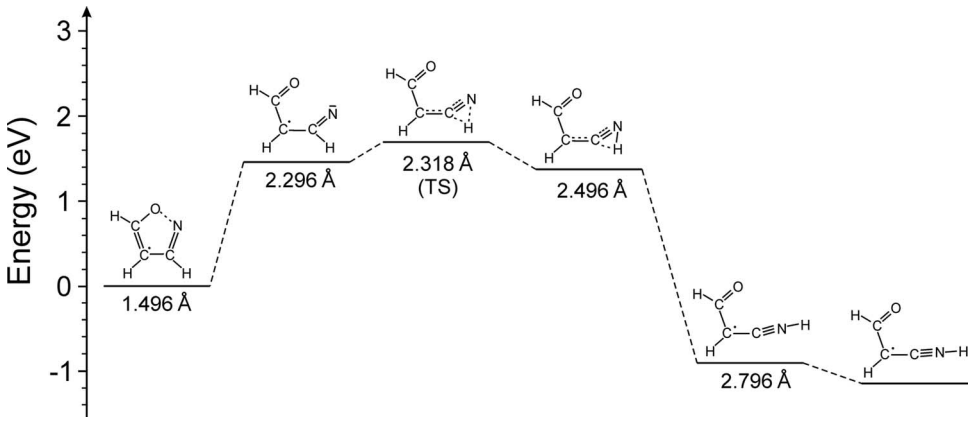

FIG. 7. The calculated energies of the $(3a'')^{-1}$ A″ cation geometries of the isoxazole molecule shown for given selected values of the N–O distance and their schematic geometries.

are shown in Fig. 7 for selected values of the N–O distance. The energy of the open ring structure increases with the N–O distance up to 2.318 Å, where the cation takes geometry of the TS with the maximum energy of 1.690 eV. After passing the saddle point, the cation energy starts to decrease, while the hydrogen atom shifts to approach the N atom. At 2.496 Å it takes an intermediate position between the C and N atoms at distances of 1.333 and 1.165 Å from them, respectively (Fig. 7). Above 2.5 Å we observe a barrierless proton transfer to form the N–H bond and further decrease of the cation energy. At 2.796 Å the cation energy is lower by 2.651 eV than that of the TS (Fig. 7). Further increase of the frozen N–O distance lowers gradually the optimized cation energy. When the N–O distance is unfrozen at 3.3 Å, the H-transferred conformation optimizes into planar open geometry with the N–H and C≡N bond lengths of 1.011 and 1.143 Å, respectively, and approximately linear C–C≡N–H chain structure. It is expected that analogous dynamics for hydrogen (proton) transfer will occur in the Rydberg superexcited states enabling to create NH fragments by subsequent cleavage of the C≡N bond.

Analogous, fully optimized calculations performed for geometry of the $(12a')^{-1}$ cation of the A′ symmetry (15.697 eV) showed electronic relaxation of the cation into the lowest energy A′ symmetry stable state, whose computed energy is 0.914 eV higher than that of the A″ symmetry. The equilibrium N–O bond length in the A′ cation (1.332 Å) is significantly shorter than in the A″ cation (1.4965 Å), hence, when the frozen N–O length is increased the energy grows faster than in the A″ symmetry. However, the orbital symmetry of the cation is not conserved and above 1.695 Å it relaxes into A″ electronic structure. Further opening of the ring follows the A″ symmetry pathway.

The appearance energy for the NH($A^3\Pi$) radicals deduced from Fig. 4 is 14.1 eV. The lowest dissociation energy limit for formation of NH($A^3\Pi$) is estimated at 12.4 eV. In this evaluation the dissociation energy calculated in the present study for the C≡N bond cleavage in the open ring isoxazole molecule is 8.84 eV. This value is comparable to the experimental CN triple bond dissociation energy.[55] The energy of the isoxazole open ring, where the NH terminates the open molecular chain, is −0.11 eV and the $A^3\Pi$ excitation energy ($\upsilon' = 0$) 3.692 eV. The higher appearance energy than that of the dissociation limit suggests existence of a reaction barrier and possible excitation of the remaining fragments of dissociation, which may also encounter translational energies. Indeed, the quantum chemical calculations[29] showed barrier of 2.5 eV.

An alternative, likely dissociation route of the superexcited states leads through autoionization into accessible cationic states, which would next dissociate yielding NH($A^3\Pi$) and the ionic particles. The estimated lowest dissociation limit for this process with autoionization into the lowest energy cationic state is 20.6 eV. This value has been obtained by combining the first ionization potential of isoxazole of 9.976 eV,[44] the calculated energy of the cation open ring structure of −1.148 eV, calculated dissociation energy of the C≡N bond in the isoxazole cation (8.107 eV), and the NH excitation energy. The energies of the observed superexcited states (Table I) are too low, for these states to follow the autoionization route. Evaluation of the dissociation limits for the dissociative direct ionization into the feasible ionic fragments, which were observed in the electron impact ionization of isoxazole,[56] gives energies above 24 eV.

V. CONCLUSIONS

Photodissociation of isoxazole molecules that produces excited NH($A^3\Pi$) free radicals has been investigated using synchrotron radiation over the 14–22 eV energy range and the photon-induced fluorescence spectroscopy. The NH($A^3\Pi$) radicals are produced through excitation of the isoxazole molecules into the higher-lying superexcited states. Observation of the NH fragment, which is not a structural unit of isoxazole molecule, demonstrates the hydrogen (proton) migration in the superexcited states prior to dissociation. The vertical excitation energies of the superexcited states were determined and the dissociation mechanisms of isoxazole were discussed. The superexcited states were correlated with the cationic ion cores, which are likely to bind the excited Rydberg electrons. The *ab initio* and density functional quantum chemical calculations suggests that the hydrogen migration

process in the molecule may be determined by the dynamical behavior of the ion core binding the Rydberg electrons in the superexcited states of the molecules.

Most of the previous investigations concentrated on studies of the hydrogen (proton) migration in molecular cations and dications under intense laser fields or in neutral species excited to lower-lying states. In the present work migration is observed for the first time in dissociation of the superexcited states of the neutral molecules excited by absorption of the VUV photon.

ACKNOWLEDGMENTS

The authors would like to acknowledge technical support from staff of the Synchrotron Trieste. The computations were performed at the Academic Computer Centre TASK in Gdańsk. One of us (I.D.) is a recipient of the FNP fellowship POMOST. This work was conducted within the framework of the COST Action CM1301 (CELINA).

[1]H. F. Schaefer III, Acc. Chem. Res. **12**, 288 (1979).
[2]H. Xu, T. Okino, K. Nakai, and K. Yamanouchi, *Progress in Ultrafast Intense Laser Science VII*, edited by K. Yamanouchi, D. Charambidis, and D. Normand (Springer, Berlin, 2011).
[3]K. Hoshina, Y. Furukawa, T. Okino, and K. Yamanouchi, J. Chem. Phys. **129**, 104302 (2008).
[4]K. M. Ervin, J. Ho, and W. C. Lineberger, J. Chem. Phys. **91**, 5974 (1989).
[5]N. Chang, M. Shen, and C. Yu, J. Chem. Phys. **106**, 3237 (1997).
[6]J. Levin, H. Feldman, A. Baer, D. Ben-Hamu, O. Heber, D. Zajfman, and Z. Vager, Phys. Rev. Lett. **81**, 3347 (1998).
[7]M. P. Jacobson and R. W. Field, J. Phys. Chem. A **104**, 3073 (2000).
[8]R. Locht and M. Davister, Chem. Phys. **195**, 443 (1995).
[9]Y. H. Jiang, A. Rudenko, O. Herrwerth, L. Foucar, M. Kurka, K. U. Kühnel, M. Lezius, M. F. Kling, J. van Tilborg, A. Belkacem, K. Ueda, S. Düsterer, R. Treusch, C. D. Schröter, R. Moshammer, and J. Ullrich, Phys. Rev. Lett. **105**, 263002 (2010).
[10]M. E. Madjet, Z. Li, and O. Vendrell, J. Chem. Phys. **138**, 094311 (2013).
[11]T. Osipov, C. L. Cocke, M. H. Prior, A. Landers, Th. Weber, O. Jagutzki, L. Schmidt, H. Schmidt-Böcking, and R. Dörner, Phys. Rev. Lett. **90**, 233002 (2003).
[12]T. S. Zyubina, Y. A. Dyakov, S. H. Lin, A. D. Bandrauk, and A. M. Mebel, J. Chem. Phys. **123**, 134320 (2005).
[13]A. Hishikawa, A. Matsuda, M. Fushitani, and E. J. Takahashi, Phys. Rev. Lett. **99**, 258302 (2007).
[14]A. Hishikawa, A. Matsuda, E. J. Takahashi, and M. Fushitani, J. Chem. Phys. **128**, 084302 (2008).
[15]H. Hasegawa, A. Hishikawa, and K. Yamanouchi, Chem. Phys. Lett. **349**, 57 (2001).
[16]T. Okino, Y. Furukawa, P. Liu, T. Ichikawa, R. Itakura, K. Hoshina, K. Yamanouchi, and H. Nakano, Chem. Phys. Lett. **423**, 220 (2006).
[17]H. Xu, C. Marceau, K. Nakai, T. Okino, S.-L. Chin, and K. Yamanouchi, J. Chem. Phys. **133**, 071103 (2010).
[18]H. Xu, T. Okino, and K. Yamanouchi, J. Chem. Phys. **131**, 151102 (2009).
[19]H. Xu, T. Okino, K. Nakai, K. Yamanouchi, S. Roither, X. Xie, D. Kartashov, M. Schöffler, A. Baltuska, and M. Kitzler, Chem. Phys. Lett. **484**, 119 (2010).
[20]S.-H. Lee, Y. T. Lee, and X. Yang, J. Chem. Phys. **120**, 10992 (2004).
[21]W. Fuß, W. E. Schmid, and S. A. Trushin, Chem. Phys. **316**, 225 (2005).
[22]K. M. Morgan, M. J. O'Connor, J. L. Humphrey, and K. E. Buschman, J. Org. Chem. **66**, 1600 (2001).
[23]A. C. Davis, N. Tangprasertchai, and J. S. Francisco, Chem. Eur. J. **18**, 11296 (2012).
[24]"Comprehensive heterocyclic chemistry," *The Structure, Reactions, Synthesis and Uses of Heterocyclic Compounds*, edited by K. T. Potts (Pergamon Press, Oxford, 1984), Vol. 6, Part 4B.
[25]A. Yokoya, N. Shikazono, K. Fujii, A. Urushibara, K. Akamatsu, and R. Watanabe, Radiat. Phys. Chem. **77**, 1280 (2008).
[26]B. Boudaiffa, P. Cloutier, D. Hunting, M. A. Huels, and L. Sanche, Science **287**, 1658 (2000).
[27]A. Lifshitz and D. Wohlfeiler, J. Phys. Chem. **96**, 4505 (1992).
[28]G. I. Yranzo and E. L. Moyano, Curr. Org. Chem. **8**, 1071 (2004).
[29]C. M. Nunes, I. Reva, T. M. V. D. Pinho e Melo, R. Fausto, T. Šolomek, and T. Bally, J. Am. Chem. Soc. **133**, 18911 (2011).
[30]K. Okada and K. Saito, J. Phys. Chem. **100**, 9365 (1996).
[31]J. Higgins, X. Zhou, and R. Liu, J. Phys. Chem. A **101**, 7231 (1997).
[32]G. E. Davico, J. Phys. Org. Chem. **18**, 434 (2005).
[33]T. J. Wasowicz, A. Kivimäki, M. Coreno, and M. Zubek, J. Phys. B **45**, 205103 (2012).
[34]I. Linert, I. Lachowicz, T. J. Wasowicz, and M. Zubek, Chem. Phys. Lett. **498**, 27 (2010).
[35]T. J. Wasowicz, A. Kivimäki, M. Dampc, M. Coreno, M. de Simone, and M. Zubek, Phys. Rev. A **83**, 033411 (2011).
[36]A. Ehresmann, S. Machida, M. Ukai, K. Kameta, M. Kitajima, N. Kouchi, Y. Hatano, K. Ito, and T. Hayaishi, J. Phys. B **28**, 5283 (1995).
[37]C. Lee, W. Yang, and R. G. Parr, Phys. Rev. B **37**, 785 (1988).
[38]R. Ditcheld, W. J. Hehre, and J. A. Pople, J. Chem. Phys. **54**, 724 (1971).
[39]M. Head-Gordon, J. A. Pople, and M. J. Frisch, Chem. Phys. Lett. **153**, 503 (1988).
[40]A. A. El-Azhary and H. U. Suter, J. Phys. Chem. **99**, 12751 (1995).
[41]E. G. Robertson, J. Mol. Spectrosc. **231**, 50 (2005).
[42]L. S. Cederbaum and W. Domcke, Adv. Chem. Phys. **36**, 205 (1977).
[43]A. D. Baker, D. Betteridge, N. R. Kemp, and R. E. Kirby, Anal. Chem. **42**, 1064 (1970).
[44]M. Dampc, B. Mielewska, M. R. F. Siggel-King, G. C. King, B. Sivaraman, S. Ptasinska, N. Mason, and M. Zubek, Chem. Phys. **367**, 75 (2010).
[45]H. B. Schlegel, J. Comput. Chem. **3**, 214 (1982).
[46]C. Peng and H. B. Schlegel, Israel J. Chem. **33**, 449 (1993).
[47]M. J. Frisch, G. W. Trucks, H. B. Schlegel *et al.*, GAUSSIAN 03, Gaussian, Inc., Wallingford, CT, 2003.
[48]C. R. Brazier, R. S. Ram, and P. F. Bernath, J. Mol. Spectrom. **120**, 381 (1986).
[49]R. L. Platzman, Radiat. Res. **17**, 419 (1962).
[50]Y. Hatano, Phys. Rep. **313**, 109 (1999).
[51]H. Nakamura, Int. Rev. Phys. Chem. **10**, 123 (1991).
[52]I. C. Walker, M. H. Palmer, J. Delwiche, S. V. Hoffmann, P. Limao Viera, N. J. Mason, M. F. Guest, M.-J. Hubin-Franskin, J. Heinesch, and A. Giuliani, Chem. Phys. **297**, 289 (2004).
[53]E. V. Gromov, C. Lévêque, F. Gatti, I. Burghardt, and H. Köppel, J. Chem. Phys. **135**, 164305 (2011).
[54]T. Fuji, Y.-I. Suzuki, T. Hario, T. Suzuki, R. Mitrić, U. Werner, and V. Bonačić-Koutecký, J. Chem. Phys. **133**, 234303 (2010).
[55]D. Shi, H. Liu, X. Zhang, J. Sun, Z. Zhu, and Y. Liu, J. Mol. Struct.:THEOCHEM **956**, 10 (2010).
[56]G. Bouchoux and Y. Hoppilliard, Org. Mass Spectrom. **16**, 459 (1981).